Lipoxins Protect Against Inflammation in Diabetes-Associated Atherosclerosis

Eoin P. Brennan,[1,2] Muthukumar Mohan,[2,3] Aaron McClelland,[2] Monica de Gaetano,[1] Christos Tikellis,[2,3] Mariam Marai,[1] Daniel Crean,[4] Aozhi Dai,[2,3] Ophelie Beuscart,[2] Sinda Derouiche,[2] Stephen P. Gray,[2] Raelene Pickering,[2,3] Sih Min Tan,[2,3] Molly Godson-Treacy,[5] Stephen Sheehan,[5] Joseph F. Dowdall,[5] Mary Barry,[5] Orina Belton,[6] Syed Tasadaque Ali-Shah,[7] Patrick J. Guiry,[7] Karin Jandeleit-Dahm,[2,3] Mark E. Cooper,[2,3] Catherine Godson,[1] and Phillip Kantharidis[2,3]

Diabetes 2018;67:2657–2667 | https://doi.org/10.2337/db17-1317

Increasing evidence points to the fact that defects in the resolution of inflammatory pathways predisposes individuals to the development of chronic inflammatory diseases, including diabetic complications such as accelerated atherosclerosis. The resolution of inflammation is dynamically regulated by the production of endogenous modulators of inflammation, including lipoxin A4 (LXA_4). Here, we explored the therapeutic potential of LXA_4 and a synthetic LX analog (Benzo-LXA_4) to modulate diabetic complications in the streptozotocin-induced diabetic $ApoE^{-/-}$ mouse and in human carotid plaque tissue ex vivo. The development of diabetes-induced aortic plaques and inflammatory responses of aortic tissue, including the expression of *vcam-1*, *mcp-1*, *il-6*, and *il-1β*, was significantly attenuated by both LXA_4 and Benzo-LXA_4 in diabetic $ApoE^{-/-}$ mice. Importantly, in mice with established atherosclerosis, treatment with LXs for a 6-week period, initiated 10 weeks after diabetes onset, led to a significant reduction in aortic arch plaque development (19.22 ± 2.01% [diabetic]; 12.67 ± 1.68% [diabetic + LXA_4]; 13.19 ± 1.97% [diabetic + Benzo-LXA_4]). Secretome profiling of human carotid plaque explants treated with LXs indicated changes to proinflammatory cytokine release, including tumor necrosis factor-α and interleukin-1β. LXs also inhibited platelet-derived growth factor–stimulated vascular smooth muscle cell proliferation and transmigration and endothelial cell inflammation. These data suggest that LXs may have therapeutic potential in the context of diabetes-associated vascular complications.

The major macrovascular complication of diabetes involves progressive cardiovascular disease (CVD) leading to diabetes-accelerated atherosclerosis (DAA), myocardial infarction, and stroke (1).

In diabetes, the mortality from CVD is twice that observed in the general population, leading to an increased incidence of atherosclerosis (2–4). Within the atherosclerotic lesion, the cellular processes driving plaque development and progression include the activation of vascular smooth muscle cells (SMCs) and endothelial cells (ECs), and monocytes. Key molecular drivers of lesion development include proinflammatory cytokines such as tumor necrosis factor-α (TNF-α), interleukin (IL)-1β, and IL-6, and also growth factors such as platelet-derived growth factor (PDGF-BB/DD) (5).

Under physiological conditions, inflammation is a finite process mediated in part by cytokines, chemokines, and lipid mediators, including prostaglandins and leukotrienes,

[1]UCD Diabetes Complications Research Centre, UCD Conway Institute of Biomolecular and Biomedical Research, UCD School of Medicine, University College Dublin, Dublin, Ireland
[2]JDRF Danielle Alberti Memorial Centre for Diabetes Complications, Diabetes Division, Baker Heart and Diabetes Institute, Melbourne, Australia
[3]Department of Diabetes, Central Clinical School, Monash University, Clayton, Victoria, Australia
[4]UCD School of Veterinary Medicine, University College Dublin, Dublin, Ireland
[5]Department of Vascular Surgery, St. Vincent's University Hospital, Dublin, Ireland
[6]School of Biomolecular and Biomedical Science, University College Dublin, Dublin, Ireland
[7]Centre for Synthesis and Chemical Biology, UCD School of Chemistry and Chemical Biology, University College Dublin, Dublin, Ireland

Corresponding author: Phillip Kantharidis, phillip.kantharidis@monash.edu.

Received 31 October 2017 and accepted 30 August 2018.

This article contains Supplementary Data online at http://diabetes.diabetesjournals.org/lookup/suppl/doi:10.2337/db17-1317/-/DC1.

E.P.B. and M.Mo. contributed equally and share equal first authorship.

M.E.C., C.G., and P.K. are co–senior authors.

which induce the migration of polymorphonuclear leukocytes (neutrophils and eosinophils) to the site of tissue damage. This initial proinflammatory phase is followed by a proresolution phase, which is characterized by the prevention of polymorphonuclear leukocyte infiltration, macrophage-mediated efferocytosis, and, ultimately, the return to tissue homeostasis. Although it is clear that inflammation plays an important role in the pathophysiology of many common diseases, including diabetes and CVD, it is now apparent that the resolution of inflammation is dynamically regulated by the production of endogenous modulators of inflammation (6–12). These specialized proresolving mediators include the ω3-derived protectins, resolvins, and maresins as well as the ω6-derived lipoxins (LXs) LXA_4 and LXB_4 (13). Indeed, we and others (14–17) have proposed that it is the failed resolution of inflammation that contributes to the pathogenesis of CVD, diabetes, and associated complications. As a result, endogenous proresolution molecules and synthetic analogs are suggested as a therapeutic strategy to promote the resolution of chronic inflammation and disease (18–20).

LXA_4 is an eicosanoid generated during acute inflammatory responses that promotes the resolution of inflammation, acting via the G-protein–coupled receptor ALX/FPR2 (21). Here we have explored the potential of LXA_4 and a synthetic analog, Benzo-LXA_4, to modulate vascular complications of diabetes in a murine model (streptozotocin [STZ]-treated $ApoE^{-/-}$ mice) (22). This model is widely used to study the effects of therapeutic agents on diabetic complications, mimicking the complex vascular lesions associated with diabetes (23,24). We then expand and confirm our findings in human carotid plaque tissue ex vivo and in in vitro models.

We report that LXs attenuate the development of atherosclerotic lesions in diabetic mice. Most noteworthy are our data that show that LXs attenuate the progression of established atherosclerotic lesions. We have also investigated the underlying mechanism of LX action in vascular tissues and found that LXs attenuate PDGF-stimulated vascular SMC proliferation and migration and EC activation. The therapeutic potential of LXs was highlighted by the inhibition of proinflammatory cytokine release from human carotid plaque explants ex vivo. These results provide insights into the pathophysiology of vascular damage as observed in atherosclerosis, particularly in the diabetes setting, and identify LXs as a novel therapeutic target for diabetic complications.

RESEARCH DESIGN AND METHODS

In Vivo Preclinical Studies

Animals were housed at the Baker Heart and Diabetes Institute and studied according to National Health and Medical Research Council (NHMRC) guidelines in line with international standards. Animals had unrestricted access to water and feed, and were maintained on a 12-h light/dark cycle on standard mouse chow (Barastoc; Ridley Agriproducts, St. Arnaud, Victoria, Australia). Six-week-old $ApoE^{-/-}$ male mice (C57BL/6 background) were rendered diabetic by five daily intraperitoneal injections of STZ (Sigma-Aldrich, St. Louis, MO) at a dose of 55 mg/kg. $ApoE^{-/-}$ mice were administered either ethanol (0.1%), LXA_4 (5 μg/kg; Merck, Calbiochem), or Benzo-LXA_4 (1.7 μg/kg; synthesized at University College Dublin [25]) twice weekly by i.p. injection. For the prevention study design, mice were followed for 10 weeks (moderate disease) or 20 weeks (severe disease), and were administered ethanol, LXA_4, or Benzo-LXA_4 between weeks 1 and 10 and weeks 1–20, respectively. For the intervention study design, mice were followed for 16 weeks, and were administered ethanol, LXA_4, or Benzo-LXA_4 between weeks 10 and 16. Blood glucose levels were monitored weekly after STZ injections for the duration of the studies to confirm the diabetic status of these mice. Only animals with a blood glucose level >15 mmol/L 1 week after the induction of diabetes were included in the study. Ten weeks after the induction of diabetes, systolic blood pressure was assessed by noninvasive tail cuff system in conscious mice. Urine samples were collected in a metabolic cage for 24 h before the end of the experiment. Glycated hemoglobin (HbA_{1c}) was measured using the Cobas Tina-quant Hemoglobin A1c Gen.3 Assay (Roche Australia, Melbourne, Victoria, Australia). Total glucose, cholesterol, and triglyceride concentrations were measured in plasma with a standard commercial enzymatic assay (Beckman Coulter Diagnostics, Gladsville, New South Wales, Australia). At the study end point, animals were anesthetized by sodium pentobarbitone (100 mg/kg i.p. body weight; Euthatal; Sigma-Aldrich, Castle Hill, New South Wales, Australia) and organs were rapidly dissected.

In Vitro Studies

Mouse primary vascular SMCs were cultured at 37°C in a humidified atmosphere of 95% air/5% CO_2, and maintained in DMEM (Life Technologies) supplemented with 25 mmol/L glucose with 10% (v/v) FBS. For treatments, media contained only 1% FBS. Mouse primary aortic ECs were maintained and passaged in 1:1 DMEM (Thermo Fisher Scientific) and Ham's F12 (Thermo Fisher Scientific) and supplemented with 10% (v/v) heat-inactivated FBS, EC growth supplement (Sigma), heparin, and 5 mmol/L D-glucose. After serum restriction for 24 h, cells were stimulated with vehicle (0.1% ethanol), LXA_4 (0.1 nmol/L; Merck, Calbiochem), or Benzo-LXA_4 (1 nmol/L) for 30 min, and media were removed and replaced with media with or without PDGF (10 ng/mL; R&D Systems), TNF-α (1 ng/mL; R&D Systems), or TGF-β1 (10 ng/mL; PromoCell GmbH). Cell experiments were performed four to six times, and the values presented are the mean ± SEM from independent experiments.

Nuclear Factor-κB Activation Analyses

Nuclear factor-κB (NF-κB) activity was assessed by transfecting SMCs with an NF-κB reporter plasmid (pNF-κB-SEAP Vector; Takara/Clontech) for 24 h, and subsequently stimulating SMCs with TNF-α for 24 h in the presence or

absence of vehicle (0.1% ethanol), LXA_4 (0.1 nmol/L; Merck, Calbiochem), or Benzo-LXA_4 (1 nmol/L). NF-κB activity was determined by measuring secreted alkaline phosphatase in culture supernatant using the SEAP Reporter Gene Assay System (Roche Australia).

Gene Expression Analyses by Reverse Transcriptase Quantitative PCR

RNA was extracted from whole mouse aorta tissue, SMCs and ECs using TRIzol (Ambion). DNase treatment and cDNA synthesis were performed as previously described (26). Gene expression was determined using TaqMan reagents (Life Technologies) with fluorescence signals being normalized to 18S rRNA or Gapdh using the ddCT method. Probes and primers were designed using a Primer Express program and were purchased from Applied Biosystems (Foster City, CA). Where no probes were used, the Fast SYBR Green Mastermix was used with gene-specific primers. Primer and probe sequences are detailed in Supplementary Table 3.

Transwell Migration Assay

SMCs were cultured as described above for 24 h, after which cells were maintained in serum restricted (1% FBS) for 24 h. After serum restriction, SMCs were either untreated or stimulated with LXA_4 (0.1–10 nmol/L; 30 min). SMCs were gently trypsinized (0.05% trypsin) and applied to gelatin-coated Transwell cell culture inserts (10 μm pore size; Corning), and PDGF (10 ng/mL) was added to relevant wells for 6 h. After this, unmigrated SMCs were gently removed from the top side of the membrane insert, and migrated SMCs on the underside of the membrane insert were fixed in ice-cold methanol and stained with 1% crystal violet. The number of migrated cells was calculated under microscope (20×), with 12 representative images taken per transwell insert.

Endothelial-Monocyte Adhesion Assay

ECs were cultured as described above for 24 h, after which cells were maintained in serum-restricted media (1% FBS) for 24 h. After serum restriction, SMCs were either untreated or stimulated with LXA_4 (0.1 nmol/L; 30 min). The human acute monocytic leukemia cell line THP-1 was obtained from the European Collection of Cell Cultures. The cells were kept in a humidified atmosphere at 37°C in the presence of 5% CO_2 and maintained in RPMI 1640 medium (Thermo Fisher Scientific) containing 11 mmol/L glucose and supplemented with 10% FBS and 2 mmol/L glutamine. Cells were stained using a CellVue Burgundy Fluorescent Cell Labeling Kit (Li-Cor). After staining, labeled THP-1 cells were cocultured with SMCs for 20 min at 37°C, nonadherent cells were gently washed, and adherent cells were counted using the Odyssey Imaging System (Li-Cor) to determine the area of fluorescent intensity. Cell experiments were performed three to six times, and the presented values are mean ± SEM values from independent experiments. Raw data are available in Supplementary Fig. 9.

Human Carotid Endarterectomy

The recruitment of individuals without diabetes and with diabetes for carotid endarterectomies was carried out at the Alfred Hospital (Melbourne, Victoria, Australia). Ethics approval was obtained from the Alfred Human Research Ethics Committee (authorization #24/07). The recruitment of donor carotid endarterectomy specimens for ex vivo assays was performed at St. Vincent's University Hospital. This study was approved by the Ethics Committee of St. Vincent's University Hospital, in accordance with International guidelines. Informed consent was obtained from all participants. Diseased carotid artery tissue was removed during the carotid endarterectomy procedure from patients with significant arterial stenosis and immediately stored in saline. Plaque processing and dissection were performed as previously described (27–29). Briefly, gross analysis was performed to assess the lesion morphology macroscopically (calcified, lipid rich, ruptured, thrombus, fibrosis). Plaque tissue was dissected into homologous small pieces (3 × 3 × 3 mm) and maintained in RPMI medium (Thermo Fisher Scientific) supplemented with 10% (v/v) FBS, 100 units/mL penicillin G, and 100 g/mL streptomycin in 24-well cell culture plates. Plaque tissue was either untreated or treated with lipopolysaccharide (LPS) (1 μg/mL; 24 h) and/or LXA_4 pretreatments (1 nmol/L, 100 nmol/L, 1 μmol/L; 30 min), and incubated at 37°C in a humidified atmosphere of 95% air/5% CO_2. Cytokines released from plaques into the culture media were quantified by ELISA using the Human ProInflammatory 7-Plex Tissue ELISA Culture Kit (MSD). The Proteome Profiler Human XL Cytokine Array Kit (R&D Systems) was used to detect the secreted levels of 105 proteins, as listed in Supplementary Figs. 6 and 7. A pooling strategy using equal volumes of supernatant (300 μL) from four carotid plaques was used to determine cytokine levels in plaques untreated or treated with LPS (1 μg/mL; 24 h) and/or LXA_4 pretreatment (100 nmol/L; 30 min). Images were quantified using ImageJ (National Institutes of Health, Bethesda, MD) and corrected for background signals of the negative controls. The mean pixel density of reference spots was set to 100, to which all other values given are relative. Heatmaps of secreted cytokine levels were generated using Morpheus (Broad Institute, Cambridge, MA).

Histological and Immunohistochemical Staining

Assessment of the aortic plaque area was undertaken using en face analysis as previously described, after staining with Sudan IV-Herxheimer solution (BDH, Poole, U.K.) (30). Digital photographs of opened aortas were obtained using a dissecting microscope (model SZX9; Olympus Optical, Tokyo, Japan) and a digital camera (Axiocam Color Camera; Carl Zeiss, North Ryde, New South Wales, Australia). The plaque area was calculated as the proportion of aortic intimal surface area occupied by red-stained plaque (Photoshop version 6.0.1; Adobe Systems, Chatswood, New South Wales, Australia). Paraffin sections (4 μm) of aorta were used to stain for Masson Trichrome, as described previously

(31,32). Sections for F4/80 were incubated with protein-blocking agent (CSA Kit; Dako) before incubation with the primary antibody anti-F4/80 (1:50, rat monoclonal anti-F4/80; Abcam) overnight at 4°C, and staining was also amplified further using the Dako Catalyzed Signal Amplification Kit, according to the manufacturer instructions. The quantification of all staining was determined using ImageJ software (http://imagej.net/Welcome).

Statistics

All statistical analyses were performed using GraphPad Prism software. Experiments with only one treatment were assessed by Student *t* test. Experiments with multiple treatment groups were analyzed by one-way ANOVA with post hoc comparisons of group means performed by the Fisher least significant difference method. A P value of ≤ 0.05 was considered to be statistically significant. Significance between groups is indicated for each figure. Unless otherwise specified, data are shown as the mean ± SEM.

RESULTS

LXs Prevent the Development of Diabetes-Associated Atherosclerosis

We induced diabetes using low-dose STZ in ApoE$^{-/-}$ mice, which were followed for 10–20 weeks to allow the development of diabetes-associated atherosclerosis. We investigated potential protection by LXs by treating mice twice weekly via intraperitoneal injection for weeks 1–20 (Fig. 1*A*). Ten-week and 20-week time points were selected to capture moderate and severe disease phenotypes. As expected, at the end of the study all diabetic animals had lower body weights (Supplementary Table 1), elevated blood glucose levels, and elevated HbA_{1c} levels compared with their nondiabetic controls. Diabetic animals also had elevated serum levels of cholesterol, triglycerides, HDL, and LDL. The metabolic parameters were unaffected by LXs, indicating that the protective effects of LXs observed in this model are not mediated by glycemic control (Supplementary Table 1).

The aortic atherosclerotic plaque area was measured in the aortic arch as well as in the thoracic and abdominal sections of the aorta of 20-week-old nondiabetic and diabetic mice. All 20-week-old diabetic animals showed a significant increase in total atherosclerotic plaque areas, which was most prominent in the aortic arch (Fig. 1*B* and *C*). Treatment of diabetic ApoE$^{-/-}$ mice with LXA_4 or Benzo-LXA_4 attenuated the development of atherosclerotic plaques within the total aorta, aortic arch, and thoracic aorta segment compared with vehicle-treated diabetic ApoE$^{-/-}$ mice. Masson Trichrome staining of aorta sections was used to quantify the density of collagen staining within the aortic wall (Supplementary Fig. 1). Here, all 20-week-old diabetic animals that were administered vehicle showed a significant increase in collagen staining in the aortic arch, and this was significantly attenuated in diabetic ApoE$^{-/-}$ mice that were administered Benzo-LXA_4 (Supplementary Fig. 1).

Inflammation and adhesion of monocytes to the vascular wall are critical steps in the initiation and development of atherosclerosis. The expression of vascular *mcp-1*, vascular cell adhesion molecule 1 (*vcam-1*), intercellular adhesion molecule 1 (*icam-1*), IL-6 (*il-6*), and IL-1β (*il-1β*) was determined by quantitative PCR. As anticipated, the increase in *mcp-1*, *vcam-1*, *icam-1*, *il-6*, and *il-1β* expression was observed in the aorta 10 weeks after the induction of diabetes (Fig. 1*D*). These responses were attenuated by the treatment of the animals with LXA_4 and Benzo-LXA_4 (Fig. 1*D*). The expression of the LXA_4 receptor *alx/fpr2* was also increased in aortic tissue from diabetic versus nondiabetic ApoE$^{-/-}$ mice (Supplementary Fig. 2). This marked upregulation of *alx/fpr2* expression may reflect enhanced leukocyte recruitment to the site of vascular lesions in diabetic tissue, ultimately increasing receptor availability for exerting LX actions. This is in keeping with the observation that there is increased expression of the macrophage markers *f4/80* and *cd11b* in diabetic mice (Fig. 2*D*). We observed a similar trend toward increased *alx/fpr2* gene expression in carotid plaque tissue from patients with diabetes versus patients without diabetes (Supplementary Fig. 2), although this did not reach statistical significance.

LXs Attenuate Established Diabetes-Associated Atherosclerosis

Given the observations that LXs could attenuate the development of atherosclerosis, we then investigated whether LXs could impact established disease. Diabetes was induced by STZ treatment of ApoE$^{-/-}$ mice, and treatment with LXs was introduced at 10 weeks for an additional 6 weeks (16-week intervention study) (Fig. 2*A* and Supplementary Table 1). At 16 weeks, diabetic animals showed a significant increase in total atherosclerotic plaque area, which was most prominent in the aortic arch (3.91 ± 0.69% [nondiabetic ApoE$^{-/-}$] vs. 19.22 ± 2.01% [diabetic ApoE$^{-/-}$]), compared with nondiabetic controls. Importantly, the treatment of diabetic ApoE$^{-/-}$ mice with LXs from weeks 10 to 16 significantly attenuated the progression of established atherosclerotic lesions within the aortic arch compared with vehicle-treated diabetic ApoE$^{-/-}$ mice [19.22 ± 2.01% (diabetic + vehicle); 12.67 ± 1.68% (diabetic + LXA_4); 13.19 ± 1.97% (diabetic + Benzo-LXA_4)] (Fig. 2*B* and *C*). This protective effect equates to an ~30% reduction in aortic arch plaque burden in this diabetic model. The expression of markers of vascular inflammation (*icam-1*, *vcam-1*, *mcp-1*) demonstrated gene expression of these molecules in aortic tissue from diabetic mice, with significant attenuation of *vcam-1* expression in diabetic mice administered Benzo-LXA_4 (Fig. 2*D*). The expression of the pan-macrophage markers *cd11b* and *f4/80* was increased in diabetic mice. However, in diabetic mice administered either LXA_4 or Benzo-LXA_4, there was no significant increase in the expression of these markers (Fig. 2*D*). In keeping with this, F4/80 immunostaining indicated increased expression of F4/80 in diabetic

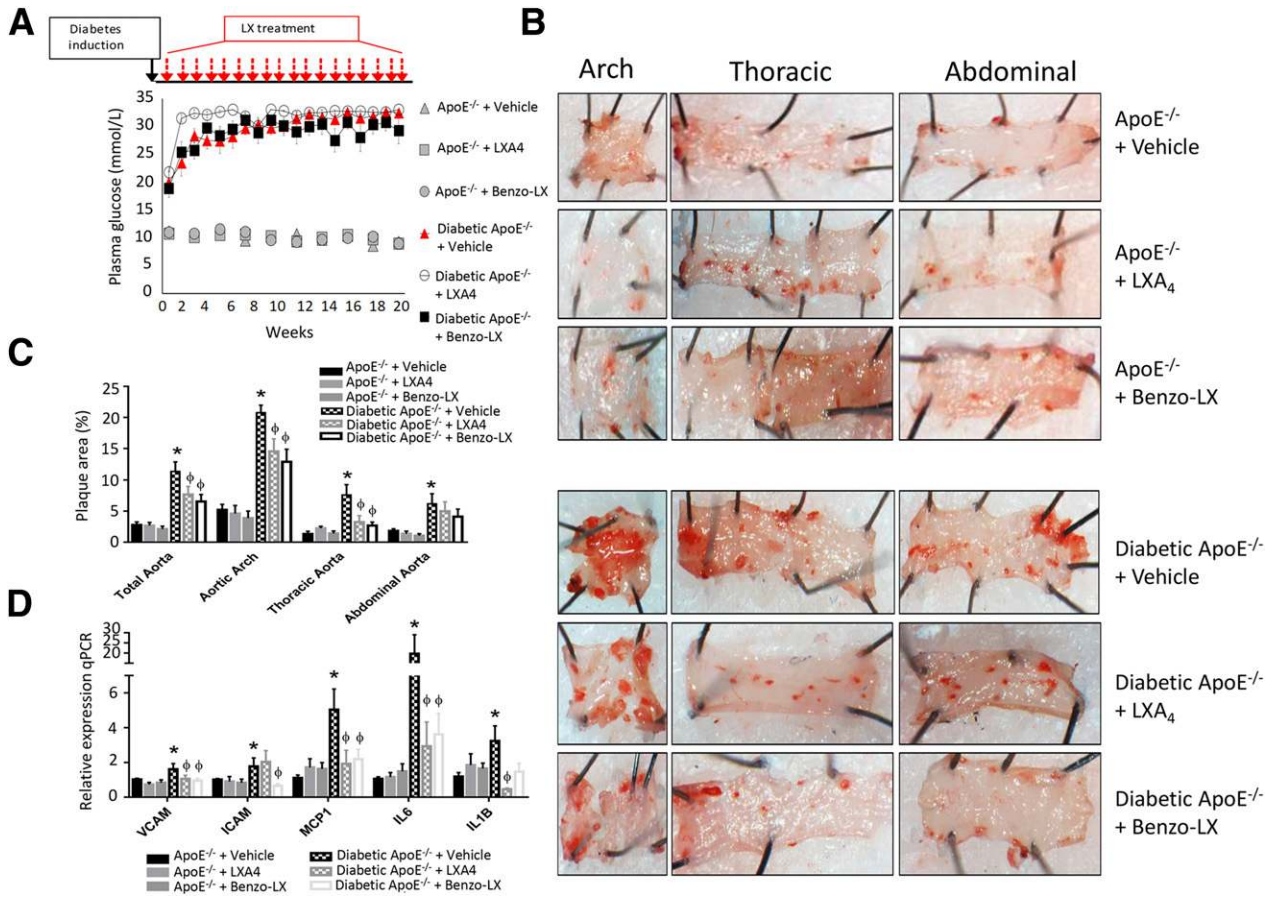

Figure 1—LXs prevent the development of diabetes-associated atherosclerosis. *A*: Averaged weekly plasma blood glucose levels in nondiabetic and diabetic ApoE$^{-/-}$ mice administered vehicle (2% ethanol), LXA_4, or Benzo-LXA_4 from weeks 1 to 16 (n = 8–10, ±SEM). *B* and *C*: Sudan IV stain of aortas isolated from 20-week-old diabetic and nondiabetic ApoE$^{-/-}$ mice administered vehicle, LXA_4, or Benzo-LXA_4, and respective quantification. N = 8–10, ±SEM; *$P \leq 0.05$ vs. ApoE$^{-/-}$ + vehicle; φ$P \leq 0.05$ vs. diabetic ApoE$^{-/-}$ + vehicle. *D*: Gene expression analysis of markers of vascular inflammation in aortic tissue isolated from 10-week-old diabetic and nondiabetic ApoE$^{-/-}$ mice administered vehicle, LXA_4, or Benzo-LXA_4. Expression was normalized to 18S for gene expression analysis (n = 8–10, ±SEM; *$P \leq 0.05$ vs. ApoE$^{-/-}$ + vehicle; φ$P \leq 0.05$ vs. diabetic ApoE$^{-/-}$ + vehicle.)

mice, and this was significantly attenuated in diabetic mice administered either LXA_4 or Benzo-LX A_4 (Supplementary Fig. 3). This would suggest that the overall macrophage content is reduced in aortic tissue of diabetic mice administered LXs. The expression of several M1 type macrophage markers (*il-6*, *il-1β*) was increased in diabetic mice, and *il-6* expression levels were not significantly upregulated in diabetic mice administered LXs. M2-type macrophage markers (*cd204*, *arg1*, and *il-10*) were also measured. Here, we observed an increase in the gene expression of these three markers in the diabetic setting (Fig. 2*D*). In diabetic aortas, the administration of Benzo-LXA_4 attenuated the upregulation of *cd204* and *arg1*, with no effect seen on *il-10* expression.

LXs and Human Atherosclerosis

To investigate the direct effects of LXs on human atherosclerotic lesions, we exposed human carotid plaque explants to LXA_4 using a previously optimized assay (29). Preliminary data established maximal cytokine release after 24 h in ex vivo culture (0–48 h) (Supplementary Fig. 4). Human plaque tissue was pretreated with LXA4 (dose range: 1 nmol/L to 1 μmol/L) or vehicle and stimulated with LPS (1 μg/mL; 24 h). LXA_4 significantly reduced IFN-γ, IL-1β, and TNF-α release, with maximal effect observed at a 100 nmol/L LXA_4 concentration, and the effect was attenuated at the higher LXA_4 concentration (1 μmol/L) (Fig. 3*A–C* and Supplementary Fig. 5). We elaborated on these data by investigating the secretion of 105 cytokines from carotid plaques (n = 4) in response to LPS and LXA_4 (100 nmol/L). Densitometric assessment of the secreted cytokines identified several cytokines regulated by LPS/LXA_4 treatments (Fig. 3*D* and *E*, Supplementary Figs. 6 and 7, and Supplementary Table 2). In particular, the levels of colony-stimulating factor 3, Regulated on Activation, Normal T Cell Expressed and Secreted (RANTES/chemokine [C-C motif] ligand [CCL] 5), and macrophage inflammatory protein 3α (CCL20) were secreted at higher levels in response to LPS priming, and this effect was mitigated by LXA_4.

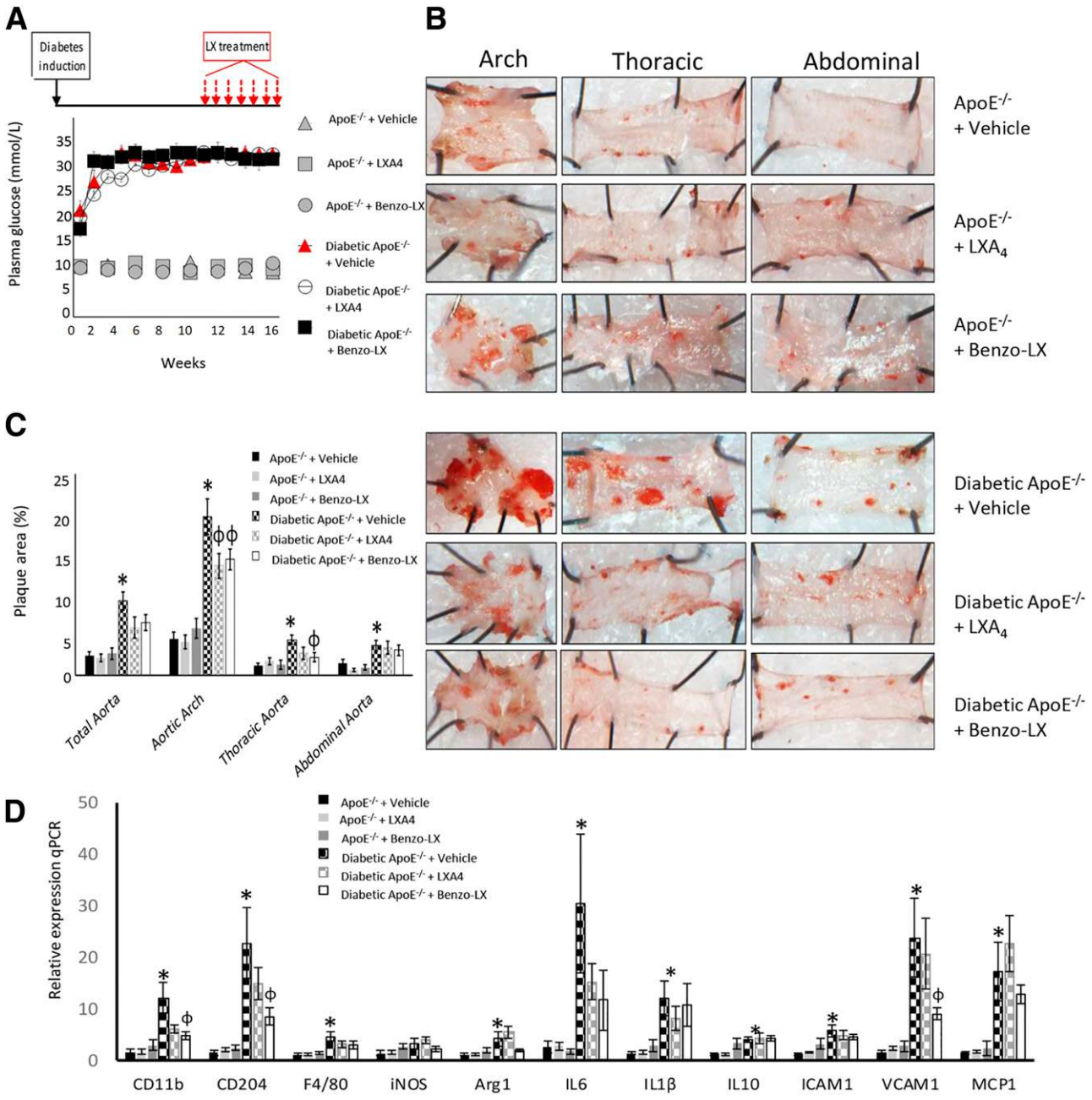

Figure 2—LXs attenuate established diabetes-associated atherosclerosis. *A*: Averaged weekly plasma blood glucose levels in nondiabetic and diabetic ApoE$^{-/-}$ mice administered vehicle (2% ethanol), LXA_4, or Benzo-LXA_4 from weeks 10 to 16 (n = 8–10, ±SEM). *B* and *C*: Sudan IV stain of aortas isolated from 16-week-old diabetic and nondiabetic ApoE$^{-/-}$ mice administered vehicle, LXA_4, or Benzo-LXA_4, and respective quantification (n = 8–10, ±SEM; *$P \leq 0.05$ vs. ApoE$^{-/-}$ + vehicle ; φ$P \leq 0.05$ vs. diabetic ApoE$^{-/-}$ + vehicle). *D*: Gene expression analysis of markers of vascular inflammation in aortic tissue isolated from 16-week-old diabetic and nondiabetic ApoE$^{-/-}$ mice administered vehicle, LXA_4, or Benzo-LXA_4 from weeks 10 to 16. Expression was normalized to 18S for gene expression analysis (n = 8–10, ±SEM; *$P \leq$ 0.05 vs. ApoE$^{-/-}$ + vehicle; φ$P \leq 0.05$ vs. diabetic ApoE$^{-/-}$ + vehicle.)

LXs Modulate Vascular Smooth Muscle Activation

PDGF plays a critical role in the regulation of SMC proliferation in atherosclerosis (23). PDGF treatment (10 ng/mL; 24 h) of SMCs induced an upregulation of several genes relevant to atherosclerotic processes, including the proliferation marker *pcna*, the cell cycle regulators *p21* and *p53*, and the growth factor receptors *pdgfr* and *tgfβ-r1* (Fig. 4*A*). Dose-response experiments were performed to identify the optimal LXA_4 dose required within the 0.1–10 nmol/L range, with 1 nmol/L LXA_4 identified as the optimal concentration (Supplementary Fig. 8). LXA_4 pretreatment (1 nmol/L; 30 min) prior to PDGF treatment, after which the RNA expression of these markers was determined. The initial LXA_4 dose response attenuated

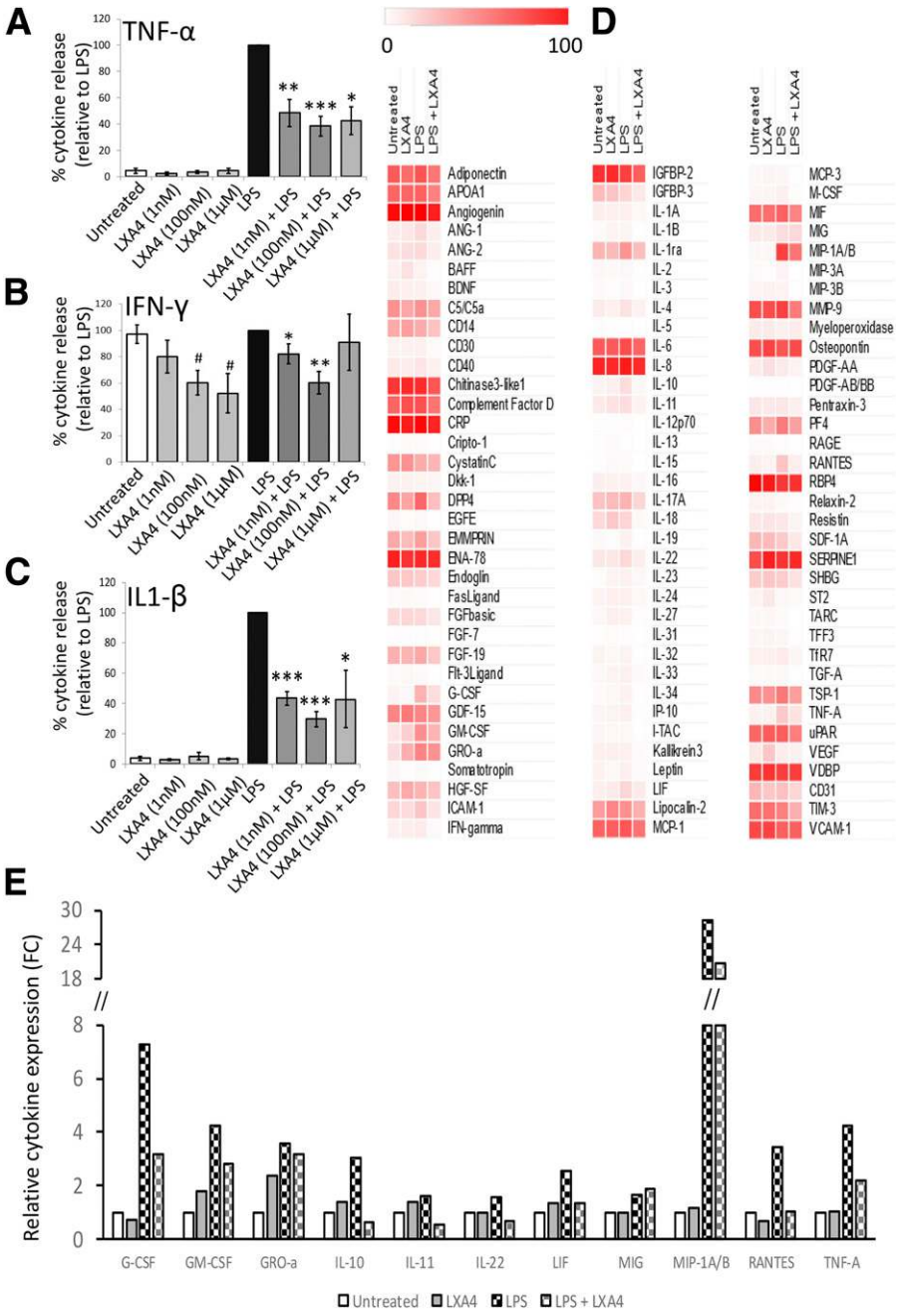

Figure 3—LXA_4 suppresses inflammatory cytokine release from human carotid plaques. *A–C*: ELISA quantification of proinflammatory cytokines released by human carotid plaques in response to LPS priming (1 μg/mL; 24 h) and or LXA_4 (1 nmol/L, 100 nmol/L, 1 μmol/L; 30 min) ($n = 4$; ±SEM; *$P \leq 0.05$ vs. LPS; **$P < 0.01$ vs. LPS; ***$P < 0.001$ vs. LPS; #$P < 0.05$ vs. untreated). Data are presented as the percentage of cytokine levels, relative to LPS-treated tissues (100%). *D*: Cytokine array analysis of secretory protein abundance of human carotid plaques ($n = 4$) in response to LPS priming (1 μg/mL; 24 h) and or LXA_4 (100 nmol/L; 30 min). The heatmap was created by setting the maximal pixel intensity of the reference spots on the array arbitrarily to 100 (red color), to which the abundance of all other analytes is relative. Minimal abundance (0) is encoded by white, maximal abundance (100) by red. *E*: Quantification of *D*, indicating fold changes (FC) of cytokines relative to untreated plaque tissue. Cytokines displaying ≥1.5-fold induction in response to LPS priming are shown. ANG, angiotensin; BDNF, brain-derived neurotrophic factor; DPP4, dipeptidyl peptidase 4; FGF, fibroblast growth factor; GRO, growth-regulated oncogene; HGF-SF, hepatocyte growth factor-scatter factor; IFN, interferon; IGF-BP, insulin-like growth factor binding protein; LIF, leukemia inhibitory factor; MIG, monokine induced by interferon-γ; RAGE, receptor for advanced glycation end products; TARC, thymus and activation regulated chemokine; TGF, transforming growth factor; TSP, thrombospondin; uPAR, urokinase plasminogen activator receptor; VDBP, vitamin D binding protein.

pcna, *p21*, *p53*, *pdgfr*, and the receptor for advanced glycation end products (*rage*), a well-validated target for diabetic complications (Fig. 4*A*). PDGF-mediated SMC migration (Fig. 4*B* and *C*) and proliferation (Fig. 4*D*) were also significantly modulated by LXA_4. SMCs upregulate an array of cellular adhesion molecules (*icam-1*, *vcam-1*) and proinflammatory cytokines in response to inflammatory stimuli such as TNF-α. We report that the

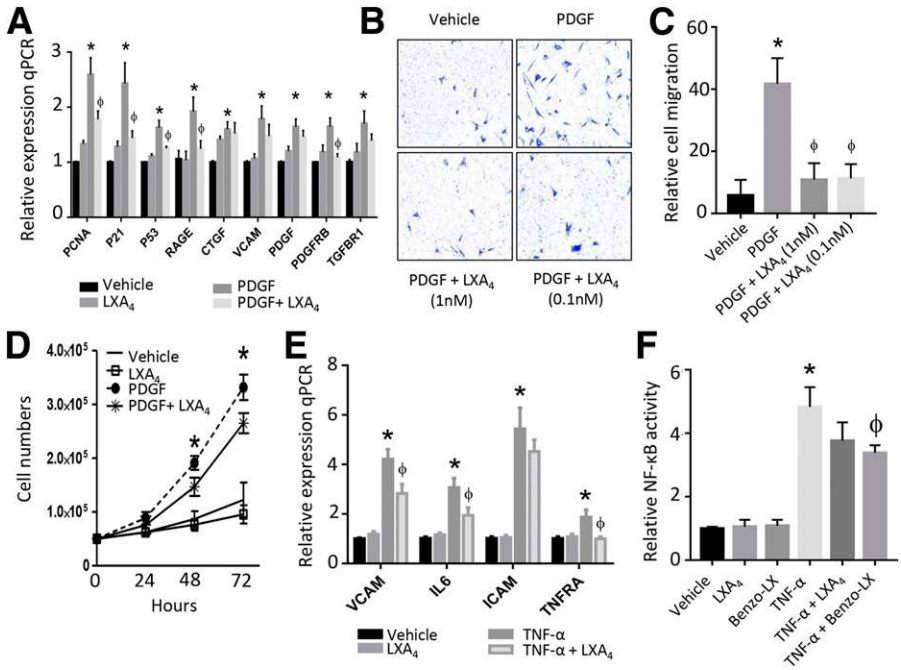

Figure 4—LXA_4 regulates vascular smooth muscle activation. *A*: Gene expression of markers of SMC activation after PDGF treatment (10 ng/mL; 24 h) and/or LXA_4 pretreatment (0.1 nmol/L; 30 min). *B* and *C*: Representative images and quantification of crystal violet–stained SMC migratory cells after PDGF treatment (10 ng/mL; 6 h) and/or LXA_4 pretreatment (0.1 nmol/L; 30 min). *D*: Cell proliferation as measured by cell number count in SMCs after PDGF treatment (10 ng/mL; 0–72 h) and/or LXA_4 pretreatment (0.1 nmol/L; 30 min). *E*: Expression of VCAM, IL-6, ICAM, and TNFR-A (TNF receptor-α) in SMCs after TNF-A treatment (1 ng/mL; 24 h) and/or LXA_4 pretreatment (0.1 nmol/L; 30 min). *F*: Luciferase/Renilla ratio results for SMCs transfected with an NF-κB activity reporter plasmid, and subsequently stimulated with TNF-α (1 ng/mL; 24 h) and/or pretreatment with LXA_4 (0.1 nmol/L; 30 min) or Benzo-LXA_4 (1 nmol/L; 30 min). Experiments were performed three to six times, and are presented as the mean ± SEM. $^*P \leq 0.05$ vs. vehicle; $\varphi P \leq 0.05$ vs. PDGF/TNF-α treatment. PCNA, proliferating cell nuclear antigen; RAGE, receptor for advanced glycation end products.

upregulation of *vcam-1*, *il-6*, and TNF-α receptor (*tnfr-α*) genes was significantly attenuated by LXA_4 (Fig. 4*E*). TNF-α is a potent inducers of NF-κB activation (11,33). Using a luciferase NF-κB promoter reporter construct, we observed a fivefold increase in NF-κB activity in SMCs in response to TNF-α (Fig. 4*F*), which was reduced by Benzo-LXA_4.

LXs Modulate Aortic EC Activation

The vascular endothelium expresses a number of adhesion molecules, including VCAM-1 and ICAM-1, which play key roles in the recruitment of leukocytes to sites of inflammation (11). Mouse primary aortic ECs were exposed to TNF-α (1 ng/mL; 24 h) in the presence/absence of LXA_4. LXA_4 inhibited TNF-α–stimulated induction of *vcam-1*, *il-6*, and *mcp-1* gene expression (Fig. 5*A*). The interaction between ECs and monocytes has an important role in the promotion of monocyte retention, foam-cell formation, and plaque formation. TNF-α significantly increases monocyte adhesion to ECs, and this interaction can be prevented by LXA_4 (Fig. 5*B* and *C*). These data further indicate that LXA_4 can suppress key inflammatory processes that contribute to endothelial dysfunction.

DISCUSSION

Targeting the resolution of inflammation represents a novel therapeutic strategy that could significantly reduce the global health burden associated with DAA. This approach is based on the postulate that strategies that promote the resolution of inflammation, such as with drugs including the LXs ,will lead to reduced end-organ damage in conditions such as diabetic complications. Interestingly, it has recently been demonstrated that circulating levels of aspirin-triggered LXA_4 (15-epi-LXA_4) are lower in patients with diabetic kidney disease versus nondiabetic kidney disease, hinting at a resolution deficit in patients with diabetic complications (34). We have shown for the first time the protective effects of LXs on vascular complications in the STZ-induced diabetic $ApoE^{-/-}$ mouse, a murine model with features of human type 1 diabetes (hyperglycemia and insulin deficiency), ultimately leading to DAA. In addition to endogenous LXA_4, we evaluated the therapeutic potential of a synthetic (1R)-stereoisomer analog (Benzo-LXA_4), generated through modification of the LXA_4 triene unit. In the current study, the Benzo-LXA_4 analog exerted similar actions to LXA_4, resulting in attenuated atherosclerotic plaque development.

To date, no studies have directly addressed the potential role of LXs as a novel therapeutic agent to reduce CVD independent of the effects on lipids, glycemic control, and/or thrombosis. Typically, vascular lesions first develop in this murine model in the aortic root and carotid arteries at 8–10 weeks of age, with more advanced lesions evident

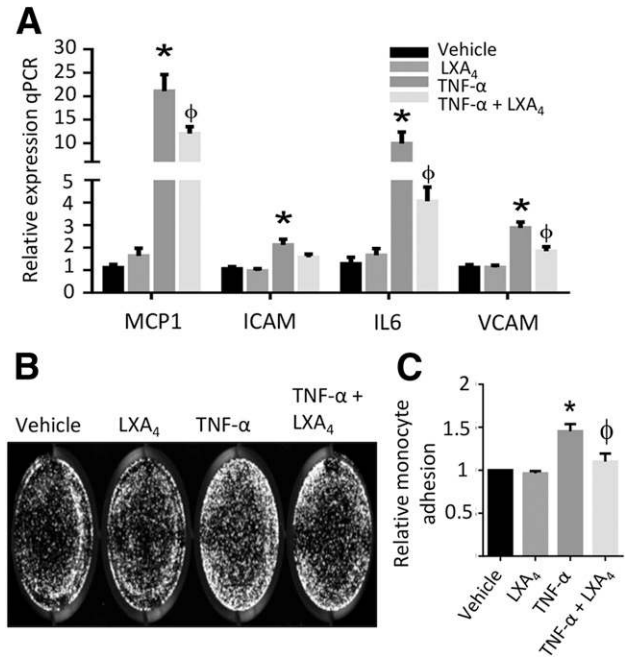

Figure 5— LXA_4 regulates aortic EC activation. *A*: Gene expression analysis of markers of vascular inflammation in aortic ECs in response to TNF-α treatment (1 ng/mL; 24 h) and/or LXA_4 pretreatment (0.1 nmol/L; 30 min). *B* and *C*: Representative images and quantification of labeled THP1 monocytes adhered to ECs stimulated with TNF-α (1 ng/mL; 24 h) and/or LXA_4 pretreatment (0.1 nmol/L; 30 min). Expression was normalized to 18S for gene expression analysis (n = 3–4, ±SEM). *$P \leq 0.05$ vs. vehicle; φ$P \leq 0.05$ vs. TNF-α treatment.

at 15 weeks (35,36). This murine model recapitulates important features of human type 1 diabetes (i.e., hyperglycemia and insulin deficiency). Here we report that blood glucose and lipid levels are unchanged by LXs in nondiabetic and diabetic mice, indicating that the protective effects of LXs are not exerted via direct control of glycemia or circulating lipid levels. In the current study, LXs attenuated the progression of DAA, inflammation, and vascular dysfunction. Crucially, the atheroprotective effect of LXs was also observed in diabetic $ApoE^{-/-}$ mice that were administered these drugs 10 weeks after the disease was established, emphasizing the utility of this therapeutic approach in subjects with established CVD, arguably the most common clinical scenario in human subjects with diabetes. It is noteworthy that the protective effect of LXs was only observed in the setting of diabetes, with no obvious effect seen in nondiabetic mice. These data would indicate that LX action is only potentiated in the setting of chronic inflammation, as observed in our diabetic mice. This is in keeping with the concept that endogenous proresolving lipid mediators, such as LXs, are typically released at the sites of inflammation, after the inflammatory response has initiated. Furthermore, It is likely that in our study, after the delivery of LXs to these mice, the inflammatory milieu seen in diabetic mice provides increased ALX/FPR2 receptor availability as a result of infiltrating leukocytes, providing the necessary machinery for LX action. In keeping with this, we show that *Alx/fpr2* expression is markedly increased in aortic tissue from diabetic mice versus nondiabetic controls, along with suggestive evidence of increased *Alx/fpr2* expression in carotid plaque tissue from patients with diabetes versus those without diabetes that further supports this hypothesis.

Our data suggest that the underlying mechanism for LX-mediated atheroprotection occurs via regulation of PDGF and TNF-α signaling in vascular cells. Excessive proliferation of vascular SMCs, macrophage infiltration, and EC dysfunction are recognized as key components of the development and progression of atherosclerosis (37). At the cellular level, our data indicate an important role for LXs in regulating PDGF-mediated SMC migration and proliferation, TNF-α–mediated NF-κB activation, and EC-monocyte interactions. We and others (38,39) have previously demonstrated that LXs exert effects on macrophages, promoting a macrophage M1-M2 switch and inhibiting macrophage apoptosis. In this model of diabetes-mediated atherosclerosis, we noted a significant increase in the expression of pan-macrophage markers *cd11b* and *f4/80* in diabetic aortic tissue, with no increase in diabetic mice administered LXs. However, we find no compelling evidence to suggest that there is a shift from M1 to M2 phenotype in response to LX treatment in this specific model; rather, the data indicate an LX-mediated effect on overall macrophage content.

In order to determine whether these molecular and cellular actions were also relevant to the human context, we further evaluated the role of endogenous LXA_4 ex vivo on human plaque lesions. LXA_4 exerted maximal effect within the 10–100 nmol/L range, with an attenuation of effect observed at the higher LXA_4 concentration (1 μmol/L). This dose-response effect is in keeping with previous studies (40–42) indicating that there is a therapeutic window for LXA_4. Among the cytokines strongly modulated by LXA_4, secretion of the glycoprotein granulocyte-macrophage colony-stimulating factor (GM-CSF) was increased in response to LPS and reduced by LXA_4. Several cytokines were released at high levels from ex vivo–treated human plaque tissue and remained unperturbed by LPS and LXA_4, including IL-6, IL-8, and CRP. This is not unexpected, given that the nature of the diseased tissue. It is possible that longer duration stimulations (2–5 days) or higher concentrations of LXs may be required to assess the therapeutic effect of these drugs on these specific highly abundant cytokines. Similarly, the sensitivity of this proteome profiler approach for detecting subtle changes in low-abundance cytokines released from plaque tissue may not be sufficient, and more accurate measurements using ELISA may be more reliable. Nevertheless, this screening strategy has identified several cytokines robustly responding to LXA_4. Interestingly, GM-CSF antagonism is currently being evaluated in several inflammatory disorders (43). Secreted levels of several additional cytokines, including CCL3/MIP1a, CCL5/RANTES, and MCP-1, all produced by various leukocyte subsets in

response to inflammatory stimuli, were also reduced by LXA_4 treatment. Thus, we demonstrate LXA_4 as an independent and effective proresolving modulator in the human plaque microenvironment building on our findings in preclinical models of atherosclerosis.

In conclusion, this study emphasizes LXs as being protective against diabetes-associated complications, such as DAA. To further clarify the role of LXs in DAA, future studies will be required to investigate the effects of LXs in models of type 2 diabetes in the presence of hyperlipidemia. Our findings warrant further experimental and clinical studies of this proresolving lipid mediator.

Acknowledgments. The authors thank the vascular surgery staff and participating patients at St. Vincent's University Hospital (Dublin, Ireland) for providing human carotid plaque material and UCD Conway Institute Core Transcriptomics Facility for technical support.

Funding. E.P.B. was supported by an ELEVATE Irish Research Council/H2020 Marie Skłodowska-Curie Actions Fellowship. This study was also supported by the NHMRC, the joint JDRF/NHMRC CRE program, and in part by the Victorian Government's Operational Infrastructure Support (OIS) Program. This work is also supported by Science Foundation Ireland, Health Research Board, and JDRF Australia awards (15/IA/3152, 15/US/B3130, and 11/PI/1206).

Duality of Interest. No potential conflicts of interest relevant to this article were reported.

Author Contributions. E.P.B. performed the experimental work, acquired and analyzed the data, designed research, and wrote, reviewed, and approved the manuscript. M.Mo., A.M., M.d.G., C.T., M.Ma., A.D., O.Beu., S.D., S.P.G., R.P., and S.M.T. performed the experimental work, acquired and analyzed the data, and reviewed and approved the manuscript. D.C. and O.Bel. reviewed and approved the manuscript. M.G.-T. performed carotid endarterectomies, provided plaque specimens and associated clinical data, performed the experimental work, acquired and analyzed the data, and reviewed and approved the manuscript. S.S., J.F.D., and M.B. performed carotid endarterectomies, provided plaque specimens and associated clinical data, and reviewed and approved the manuscript. S.T.A.-S. and P.J.G. designed and synthesized the Benzo-LXA4 analog and reviewed and approved the manuscript. K.J.-D., M.E.C., C.G., and P.K. designed research and wrote, reviewed, and approved the manuscript. E.P.B. is the guarantor of this work and, as such, had full access to all the data in the study and takes responsibility for the integrity of the data and the accuracy of the data analysis.

References

1. Haffner SM, Lehto S, Rönnemaa T, Pyörälä K, Laakso M. Mortality from coronary heart disease in subjects with type 2 diabetes and in nondiabetic subjects with and without prior myocardial infarction. N Engl J Med 1998;339:229–234
2. Kornowski R, Mintz GS, Kent KM, et al. Increased restenosis in diabetes mellitus after coronary interventions is due to exaggerated intimal hyperplasia. A serial intravascular ultrasound study. Circulation 1997;95:1366–1369
3. Tanaka N, Terashima M, Rathore S, et al. Different patterns of vascular response between patients with or without diabetes mellitus after drug-eluting stent implantation: optical coherence tomographic analysis. JACC Cardiovasc Interv 2010;3:1074–1079
4. Mäkinen VP, Forsblom C, Thorn LM, et al. Network of vascular diseases, death and biochemical characteristics in a set of 4,197 patients with type 1 diabetes (the FinnDiane Study). Cardiovasc Diabetol 2009;8:54
5. Tedgui A, Mallat Z. Cytokines in atherosclerosis: pathogenic and regulatory pathways. Physiol Rev 2006;86:515–581
6. Brennan EP, Nolan KA, Börgeson E, et al.; GENIE Consortium. Lipoxins attenuate renal fibrosis by inducing let-7c and suppressing TGFβR1. J Am Soc Nephrol 2013;24:627–637
7. Börgeson E, Godson C. Resolution of inflammation: therapeutic potential of pro-resolving lipids in type 2 diabetes mellitus and associated renal complications. Front Immunol 2012;3:318
8. Donath MY. Targeting inflammation in the treatment of type 2 diabetes: time to start. Nat Rev Drug Discov 2014;13:465–476
9. Serhan CN. Resolution phase of inflammation: novel endogenous anti-inflammatory and proresolving lipid mediators and pathways. Annu Rev Immunol 2007;25:101–137
10. Serhan CN, Savill J. Resolution of inflammation: the beginning programs the end. Nat Immunol 2005;6:1191–1197
11. Tabas I, García-Cardeña G, Owens GK. Recent insights into the cellular biology of atherosclerosis. J Cell Biol 2015;209:13–22
12. Tabas I, Glass CK. Anti-inflammatory therapy in chronic disease: challenges and opportunities. Science 2013;339:166–172
13. Spite M, Clària J, Serhan CN. Resolvins, specialized proresolving lipid mediators, and their potential roles in metabolic diseases. Cell Metab 2014;19:21–36
14. Serhan CN, Yacoubian S, Yang R. Anti-inflammatory and proresolving lipid mediators. Annu Rev Pathol 2008;3:279–312
15. Maderna P, Godson C. Lipoxins: resolutionary road. Br J Pharmacol 2009;158:947–959
16. Neuhofer A, Zeyda M, Mascher D, et al. Impaired local production of pro-resolving lipid mediators in obesity and 17-HDHA as a potential treatment for obesity-associated inflammation. Diabetes 2013;62:1945–1956
17. Fredman G, Hellmann J, Proto JD, et al. An imbalance between specialized pro-resolving lipid mediators and pro-inflammatory leukotrienes promotes instability of atherosclerotic plaques. Nat Commun 2016;7:12859
18. Perretti M. The resolution of inflammation: new mechanisms in pathophysiology open opportunities for pharmacology. Semin Immunol 2015;27:145–148
19. Fullerton JN, Gilroy DW. Resolution of inflammation: a new therapeutic frontier. Nat Rev Drug Discov 2016;15:551–567
20. Gilroy D, De Maeyer R. New insights into the resolution of inflammation. Semin Immunol 2015;27:161–168
21. Brennan EP, Cacace A, Godson C. Specialized pro-resolving mediators in renal fibrosis. Mol Aspects Med 2017;58:102–113
22. Wu KK, Huan Y. Diabetic atherosclerosis mouse models. Atherosclerosis 2007;191:241–249
23. Lassila M, Allen TJ, Cao Z, et al. Imatinib attenuates diabetes-associated atherosclerosis. Arterioscler Thromb Vasc Biol 2004;24:935–942
24. Lassila M, Jandeleit-Dahm K, Seah KK, et al. Imatinib attenuates diabetic nephropathy in apolipoprotein E-knockout mice. J Am Soc Nephrol 2005;16:363–373
25. Börgeson E, Docherty NG, Murphy M, et al. Lipoxin A_4 and benzo-lipoxin A_4 attenuate experimental renal fibrosis. FASEB J 2011;25:2967–2979
26. Kantharidis P, Hagiwara S, Brennan E, McClelland AD. Study of microRNA in diabetic nephropathy: isolation, quantification and biological function. Nephrology (Carlton) 2015;20:132–139
27. Erbel C, Okuyucu D, Akhavanpoor M, et al. A human ex vivo atherosclerotic plaque model to study lesion biology. J Vis Exp 2014;(87):e50542
28. de Gaetano M, Crean D, Barry M, Belton O. M1- and M2-type macrophage responses are predictive of adverse outcomes in human atherosclerosis. Front Immunol 2016;7:275
29. Brennan E, Wang B, McClelland A, et al. Protective effect of let-7 miRNA family in regulating inflammation in diabetes-associated atherosclerosis. Diabetes 2017;66:2266–2277
30. Watson AM, Li J, Schumacher C, et al. The endothelin receptor antagonist avosentan ameliorates nephropathy and atherosclerosis in diabetic apolipoprotein E knockout mice. Diabetologia 2010;53:192–203
31. Chai Z, Dai A, Tu Y, et al. Genetic deletion of cell division autoantigen 1 retards diabetes-associated renal injury. J Am Soc Nephrol 2013;24:1782–1792

32. Gray SP, Di Marco E, Kennedy K, et al. Reactive oxygen species can provide atheroprotection via NOX4-dependent inhibition of inflammation and vascular remodeling. Arterioscler Thromb Vasc Biol 2016;36:295–307
33. Hajra L, Evans AI, Chen M, Hyduk SJ, Collins T, Cybulsky MI. The NF-kappa B signal transduction pathway in aortic endothelial cells is primed for activation in regions predisposed to atherosclerotic lesion formation. Proc Natl Acad Sci U S A 2000;97:9052–9057
34. Goicoechea M, Sanchez-Niño MD, Ortiz A, et al. Low dose aspirin increases 15-epi-lipoxin A4 levels in diabetic chronic kidney disease patients. Prostaglandins Leukot Essent Fatty Acids 2017;125:8–13
35. Getz GS, Reardon CA. Animal models of atherosclerosis. Arterioscler Thromb Vasc Biol 2012;32:1104–1115
36. Nakashima Y, Plump AS, Raines EW, Breslow JL, Ross R. ApoE-deficient mice develop lesions of all phases of atherosclerosis throughout the arterial tree. Arterioscler Thromb 1994;14:133–140
37. Fuster JJ, Fernández P, González-Navarro H, Silvestre C, Nabah YN, Andrés V. Control of cell proliferation in atherosclerosis: insights from animal models and human studies. Cardiovasc Res 2010;86:254–264
38. Prieto P, Cuenca J, Través PG, Fernández-Velasco M, Martín-Sanz P, Boscá L. Lipoxin A4 impairment of apoptotic signaling in macrophages: implication of the PI3K/Akt and the ERK/Nrf-2 defense pathways. Cell Death Differ 2010;17:1179–1188
39. Börgeson E, Johnson AM, Lee YS, et al. Lipoxin A4 attenuates obesity-induced adipose inflammation and associated liver and kidney disease. Cell Metab 2015;22:125–137
40. Goh J, Baird AW, O'Keane C, et al. Lipoxin A(4) and aspirin-triggered 15-epi-lipoxin A(4) antagonize TNF-alpha-stimulated neutrophil-enterocyte interactions in vitro and attenuate TNF-alpha-induced chemokine release and colonocyte apoptosis in human intestinal mucosa ex vivo. J Immunol 2001;167:2772–2780
41. Chung-a-on KO, Soyombo O, Spur BW, Lee TH. Stimulation of protein kinase C redistribution and inhibition of leukotriene B4-induced inositol 1,4,5-trisphosphate generation in human neutrophils by lipoxin A4. Br J Pharmacol 1996;117:1334–1340
42. Andersson P, Serhan CN, Petasis NA, Palmblad J. Interactions between lipoxin A4, the stable analogue 16-phenoxy-lipoxin A4 and leukotriene B4 in cytokine generation by human monocytes. Scand J Immunol 2004;60:249–256
43. Wicks IP, Roberts AW. Targeting GM-CSF in inflammatory diseases. Nat Rev Rheumatol 2016;12:37–48